JBMR Plus, 2025, **9**, ziaf066
https://doi.org/10.1093/jbmrpl/ziaf066
Advance access publication: April 16, 2025
Research Article

A three-material model for dual-layer detector spectral computed tomography measurements of marrow adipose tissue and bone mineral density

Fengyun Zhou[1], Glen M. Blake[2], Zhe Guo[1], Wenshuang Zhang[1], Yi Yuan[1], Yandong Liu[1], Jian Geng[1], Bo Hu[1], Kangkang Ma[1], Zitong Cheng[1], Qingyu Zhang[1], Dong Yan[1], Xiaoguang Cheng[1,3,*], Ling Wang[1,4,*]

[1]Department of Radiology, Beijing Jishuitan Hospital, Capital Medical University, National Center for Orthopaedics, Beijing 100035, China
[2]School of Biomedical Engineering & Imaging Sciences, King's College London, St Thomas' Hospital, London SE1 7EH, United Kingdom
[3]Beijing Research Institute of Traumatology and Orthopaedics, Beijing 100035, China
[4]JST Sarcopenia Research Centre, National Center for Orthopaedics, Beijing Research Institute of Traumatology and Orthopaedics, Beijing Jishuitan Hospital, Capital Medical University, Beijing 100035, China
*Corresponding authors: Department of Radiology, Beijing Jishuitan Hospital, Capital Medical University, No. 31 Xinjiekou East Street, Xicheng District, 100035 Beijing, China (Xiaoguang Cheng, xiao65@263.net and Ling Wang, doctorwl@bjmu.edu.cn)

Abstract

Single-energy QCT (SEQCT) scans to measure volumetric BMD (vBMD) are susceptible to errors caused by variability in the amount of marrow adipose tissue (MAT). We developed a three-material model that uses dual-layer spectral CT (DLCT) technology to measure bone matrix (BM), yellow marrow (YM), and red marrow (RM) and compared the results with measurements of proton density fat fraction (PDFF) by MRI and vBMD by SEQCT. Hounsfield units (HU) were measured in the L1-3 vertebrae on 50 and 150 keV mono-energy images in a training set of 100 Chinese adults. The densities of YM and RM in the three-material model were adjusted so that the mean and SD of the YM volume as a fraction of total marrow volume matched historical bone histology data. A validation set of 125 adults was scanned, and the findings were compared with measurements of L1-3 MRI PDFF and SEQCT vBMD. We evaluated the sensitivity, specificity, and area under the ROC curve (AUROC) for DLCT vBMD measurements to predict osteoporosis and investigated the relationship between SEQCT vBMD, DLCT vBMD, and YM volume fraction. The mean (range) of the YM volume as a fraction of total marrow volume averaged 0.471 (0.190-0.674) and 0.480 (0.258-0.760) in men and women. The corresponding results for MRI PDFF were 0.487 (0.224-0.675) and 0.477 (0.238-0.745). The coefficient of determination was $r^2 = 0.696$ ($p < .0001$; SEE = 0.059). A L1-3 DLCT vBMD of 100 mg/cm^3 gave a sensitivity of 100.0% and a specificity of 94.3% for predicting osteoporosis (AUROC = 0.986). A multiple linear regression model to predict L1-3 SEQCT vBMD from DLCT vBMD and the YM fraction gave a coefficient of determination of $r^2 = 0.989$ ($p < .0001$; SEE = 5.2 mg/cm^3). In conclusion, we developed a three-material model for analyzing DLCT scans that correlates with MRI measurements of MAT PDFF and offers a potentially improved method of using CT to measure vBMD.

Keywords: spectral CT, MRI PDFF, single-energy QCT, material decomposition, BMD, marrow adipose tissue, osteoporosis, osteopenia

Lay Summary

Measurements of bone density in the spine using standard CT scans are affected by errors caused by the variations in the amount of fat in bone marrow. Dual-layer CT (DLCT) is a new type of CT scan that allows bone and fat to be measured at the same time. We developed a mathematical model that converts DLCT measurements of high- and low-energy X-rays into separate measurements of the amounts of bone and fat in the spine. We tested the model in a group of 125 patients and compared the results with MRI measurements of fat in the spine and conventional CT bone density measurements. By allowing for the fat in bone marrow, DLCT scans may provide bone density measurements that are more accurate than those measured by standard CT scans.

Received: January 23, 2025. **Revised:** March 26, 2025. **Accepted:** March 31, 2025

Graphical Abstract

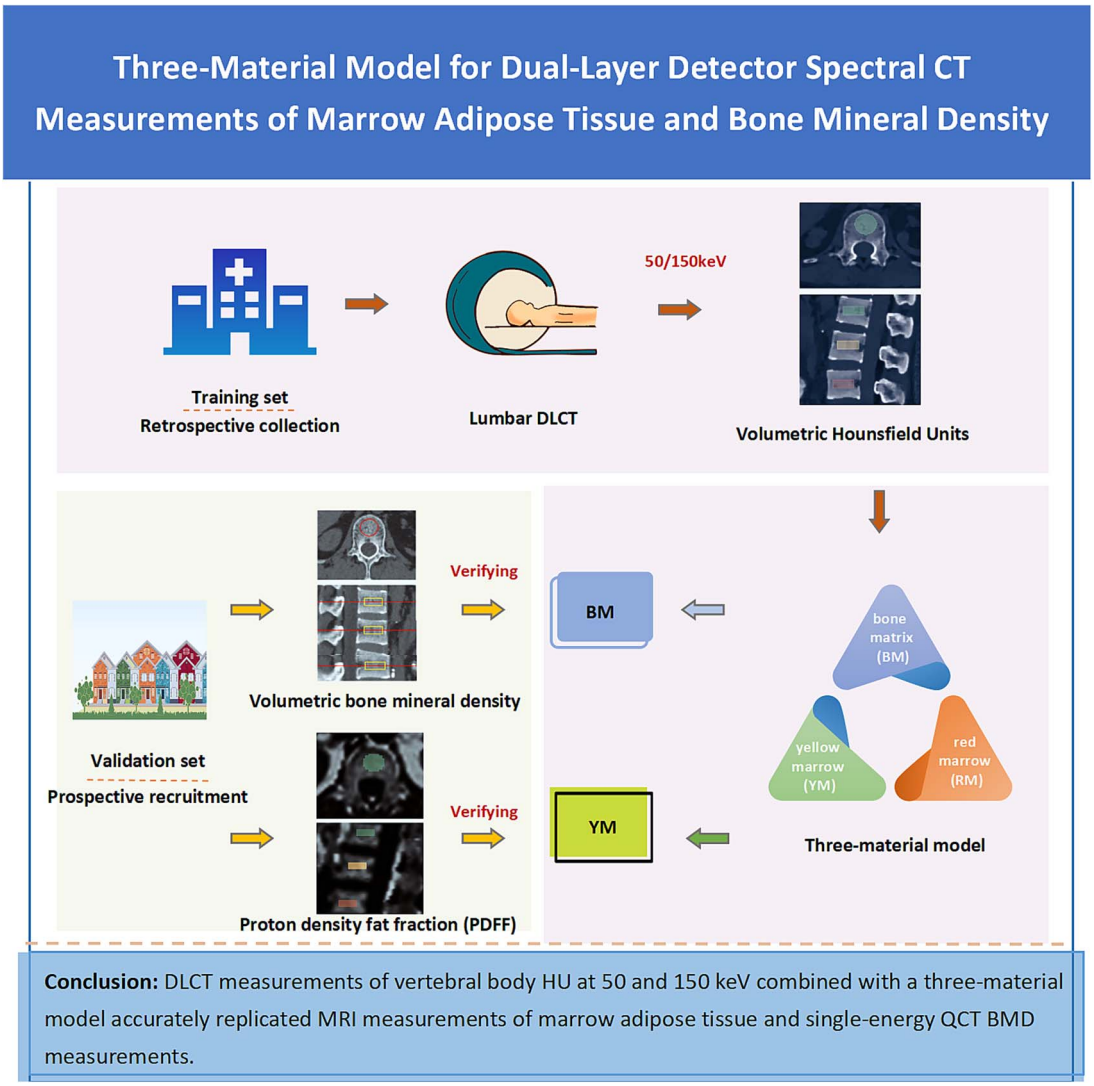

Introduction

Osteoporosis is a systemic disease of the skeleton characterized by decreased bone mass, resulting in increased bone fragility and susceptibility to fracture.[1,2] Opportunistic screening using CT imaging can play an important role in identifying individuals with low spine BMD that are at increased risk of a vertebral fracture, enabling early intervention with treatment.

Worldwide, DXA is the most widely used method for evaluating BMD. However, areal BMD (aBMD, units mg/cm^2) measured by DXA involves a 2D projection scan that is susceptible to artifacts due to degenerative changes.[3] Quantitative CT (QCT) is an alternative method of measuring BMD that overcomes the limitations of DXA by assessing the volumetric BMD (vBMD, units mg/cm^3) of trabecular bone in the lumbar vertebral bodies and shows superior sensitivity for identifying patients with osteoporosis.[4] However, conventional single-energy QCT (SEQCT) measures vBMD at a single effective photon energy and is itself susceptible to errors due to the variable amount of marrow adipose tissue (MAT). In addition, SEQCT requires the scanning of a calibration phantom, and no retrospective analysis is possible.

Dual-layer spectral CT (DLCT) is a new imaging technology that generates spectral information at the detectors and offers a variety of material-specific CT applications that include the potential to provide more accurate measurements of spine vBMD without the need for a calibration phantom.[5] By means of two superimposed layers of detectors, DLCT enables the separation of low- and high-energy photons, and by providing energy-specific information on X-ray attenuation, it enables material-specific density information to be derived.[5] Among the possible new applications, by simultaneously measuring MAT, DLCT could provide improved vBMD measurements alongside the conventional morphological assessments of CT imaging.[6]

Some studies of DLCT-based quantitative vBMD assessment have already reported on the reliability of the measurements in phantoms and patients.[6–9] However, no study has yet addressed the issue of whether DLCT can yield reliable estimates of MAT. Therefore, the objectives of the present study were to develop a three-material model for DLCT-based material decomposition of the lumbar spine that produced solutions for the YM volume consistent with historical bone histology data and to compare the resulting MAT and vBMD measurements with MRI measurements of proton density fat

Table 1. Patient characteristics in the training and validation sets.

Basic information	Training set ($n = 100$)		Validation set ($n = 125$)	
	Men ($n = 43$)	Women ($n = 57$)	Men ($n = 44$)	Women ($n = 81$)
Age (yr)[a]	51.1 (14.7)	53.5 (14.7)	53.2 (12.8)	53.7 (13.2)
Height (cm)[a]	172.3 (5.3)	160.2 (4.6)	171.7 (5.8)	161.0 (5.4)
Weight (kg)[a]	69.4 (9.3)	58.4 (7.5)	74.8 (10.5)	61.5 (13.0)
BMI (kg/m^2)[a]	23.4 (3.3)	22.7 (2.5)	25.3 (2.8)	23.7 (4.4)
SEQCT vBMD (mg/cm^3)[a]	129.5 (41.5)	120.5 (50.6)	137.9 (46.7)	132.7 (51.3)
Osteoporosis[b]	5/43	14/57	4/44	16/81
Osteopenia[c]	15/43	17/57	13/44	19/81

[a]Data expressed as the mean with the SD in parentheses. [b]Number of patients with osteoporosis defined by SEQCT L1-3 vBMD <80 mg/cm^3. [c]Number of patients with osteopenia defined by SEQCT L1-3 vBMD >80 and <120 mg/cm^3. Abbreviations: SEQCT, single-energy QCT; vBMD, volumetric BMD.

fraction (PDFF) and SEQCT measurements of spine vBMD, respectively.

Materials and methods

Participants in the training and validation sets

The study protocol was approved by our Hospital Ethics Committee (approval number: 202112-11-01) and all participants signed informed consent forms.

A training set of 100 Chinese participants was retrospectively enrolled, consisting of all the patients aged 20 yr and older referred for a non-contrast lumbar spine DLCT examination between May 2022 and August 2023 (Table 1). Patients meeting any of the following criteria were excluded from the study: (1) presence of primary or metastatic bone tumors in the spine, (2) severe scoliosis of the spine, (3) fracture involving more than 2 vertebrae, and (4) lumbar vertebrae with metallic implants following spinal surgery. The training set was used together with historical bone histology data to develop a three-material model of vertebral trabecular bone that was subsequently tested in a separate validation study. The validation set consisted of 125 Chinese participants recruited prospectively from communities close to our hospital for a non-contrast lumbar spine DLCT and a spine MR examination to measure MAT PDFF (Table 1). The exclusion criteria were the same as above. As well as measurements of Hounsfield units (HU) at specific high and low mono-energies, the DLCT scans also provided SEQCT measurements of spine vBMD. The validation set was used to verify the capability of the DLCT model to reliably predict MAT PDFF, to quantitatively compare DLCT and SEQCT vBMD measurements, and to identify osteoporosis or osteopenia by comparison with SEQCT.

DLCT and MR imaging acquisition

The lumbar spine examinations were performed using a DLCT scanner (IQon Spectral CT, Philips Healthcare). Patient examinations were performed with a standard tube voltage of 120 kV, exposure of 125 mAs, a slice thickness of 1 mm, a matrix of 512×512, and a pitch of 1. Spectral base image datasets were reconstructed using a soft tissue reconstruction kernel with an axial slice thickness of 1 mm into conventional CT images and virtual mono-energetic images at 50 and 150 keV with IntelliSpace Portal software (version 11.1.1, Philips Healthcare). The standard IQon CT images were post-processed using QCT Pro software (Mindways Software, Inc.) to generate SEQCT vBMD values. An asynchronous calibration phantom (Mindways Software, Inc.) was scanned once a week throughout the study for calibration and quality assurance.[10] In addition, 10 DLCT scans of a water phantom were performed to measure the HU values in water at 50 and 150 keV.

Q-Dixon MRI is a multi-echo, 3D, gradient echo volumetric interpolated breath-hold examination sequence utilizing T_2*-corrected, 6-point (6 pt) Q-Dixon techniques to generate water, fat, T_2*, R_2*, in-phase, and opposed-phase images.[11–13] The PDFF maps were automatically reconstructed and then processed using the open-source software 3D Slicer (version 5.0.3) for data extraction.[14] The lumbar spine imaging parameters were: an image resolution of $1.4 \times 1.4 \times 3.0$ mm^3; 104 slices; a field of view of 450×390 mm; time echoes of 1.05/2.46/3.69/4.92/6.15/7.38 ms; a repetition time of 8.82 ms; a flip angle of 4°; a bandwidth of 1080 Hz/px; one signal average; and an acquisition time of 17 s.

DLCT and MR image analysis

DLCT 50 and 150 keV mono-energy images (Figure 1A) and MR PDFF maps (Figure 1B) were imported into 3D slicer software for delineation of the VOIs in the L1-3 vertebral bodies. The VOIs were set at a height of 9 mm, and a cylindrical cross-section was drawn to be as large as possible, carefully avoiding intersection with the vertebral cortex, dense bone islands, venous plexuses, or focal lesions. In cases where a vertebral body was fractured, the adjacent vertebra was used as a substitute. For VOI delineation on the PDFF maps, high-resolution T1-weighted images were utilized to accurately localize structures, ensuring that dense bone islands, venous plexuses, and focal lesions were excluded.

For the measurement of SEQCT vBMD (mg/cm^3), all CT images were transferred to a Mindways QCT-Pro workstation for the generation and semiautomatic analysis of VOIs (Figure 1C-E). The DLCT-derived vBMD, SEQCT-derived vBMD values, and MRI PDFF were measured simultaneously to ensure consistency in terms of the VOI location, VOI size, and measured vertebrae of each participant among the three imaging measurements. VOI measurements were independently performed by 2 radiologists (LW, with 5 yr of experience, and FYZ, in-training) who were blinded to each other's findings.

DLCT spectral analysis decomposition of bone

The three-material model is illustrated in Figure 2 and a full discussion of the model is given in the Supplemental material (see Table S1 and Figures S1 and S2). In brief, the model was developed from several previously published studies.[15–18]

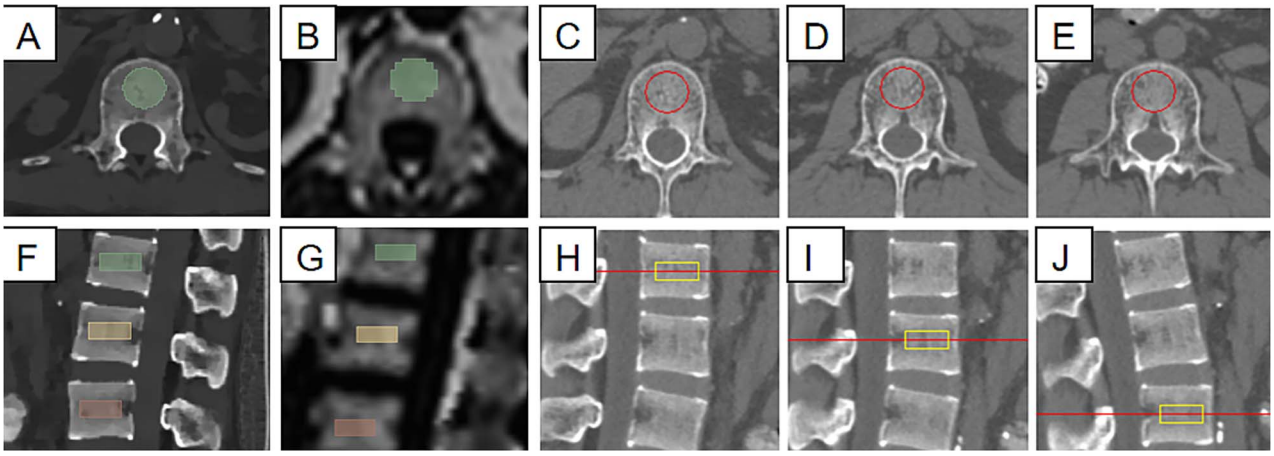

Figure 1. The volume region of interest (VOI) was defined on dual-energy spectral CT (DLCT) virtual monoenergetic images (A) and MR images (B) with 3D slicer software. Single-energy quantitative CT (SEQCT) measurements of spine volumetric BMD (vBMD) were performed on conventional non-contrast CT images (C-E). (F-J) shows the corresponding sagittal images.

The three materials in the model were: (1) bone matrix (BM), consisting of 58% by weight hydroxyapatite (HA), 32% collagen, and 10% water[15]; (2) yellow marrow (YM); and (3) red marrow (RM). The compositions of YM and RM were taken from ICRU Report 46[19] and collagen from the PubChem database.[20] Mass attenuation coefficients were taken from the NIST tables.[21] The fractional volumes of BM, YM, and RM were derived by solving three linear equations that related the linear attenuation coefficients and volumes to the HU measurements at 50 and 150 keV. The mass densities of YM and RM were treated as adjustable parameters that were fitted to the training set to ensure a mean adjusted YM fraction [Adj-YM = YM/(YM + RM)] of 0.50 with ±1.96 SD of 0.25 and 0.75.[15] These latter values are based on historical bone histology data that are independent of modern MRI measurements.

Statistical analysis

Assuming a sample size of 125 participants and a true Pearson correlation coefficient of $r = 0.80$ between the DLCT and MRI MAT measurements, the study has 90% power to detect $r = 0.66$ or greater at $p = .05$.

Normally and non-normally distributed data were expressed as mean ± SD and median (interquartile range), respectively. The correlation between variables was calculated by Pearson's correlation coefficient. Multiple linear regression analysis was used to investigate the relationship between SEQCT vBMD, DLCT vBMD, and the Adj-YM volume fraction. Osteoporosis and osteopenia were defined according to the American College of Radiology criteria based on a SEQCT L1-3 vBMD measurement of <80 mg/cm^3 and between 80 and 120 mg/cm^3, respectively.[22] Receiver operating characteristic (ROC) analysis was used to evaluate the sensitivity, specificity, positive predictive value (PPV), negative predictive value (NPV), and area under the ROC curve (AUROC) for DLCT L1-3 vBMD to predict osteoporosis and osteopenia as defined by SEQCT. As a comparison with the densities of YM and RM inferred from the training set, we used data from the validation set to calculate independent estimates of the 2 densities by equating the mean and SD of the DLCT Adj-YM volume fraction measurements to the MRI PDFF measurements. SPSS (version 26.0, IBM) and GraphPad Prism (version 8.0, GraphPad Software) were used for the statistical analyses. A p-value of less than .05 was considered to indicate a statistically significant difference.

Results

Participants' characteristics

The characteristics of participants in the training and validation sets are summarized in Table 1. Participants in the training set ranged from 20 to 85 yr old, and in the validation set, from 22 to 82 yr old. SEQCT L1-3 vBMD was included in this table since it was used to determine the numbers of men and women with osteoporosis and osteopenia. Analysis of the training set gave mass densities of 0.924 and 1.057 g/cm^3 for YM and RM, respectively, to ensure a mean Adj-YM volume fraction of 0.5 with 95% of the measurements between 0.25 and 0.75[15] (Table S1, Figure 2).

The results of the three-material decomposition of the DLCT 50 and 150 keV HU measurements for participants in the 2 datasets are shown separately in Table 2. The results are those averaged over L1-3 using the model parameters listed in Table S1. The YM volume fraction in the validation set averaged 0.416 (range 0.161-0.625) in men and 0.426 (range 0.208-0.692) in women. When expressed as a fraction of the total marrow volume, the mean Adj-YM volume fraction was 0.471 (range 0.190-0.674) and 0.480 (range 0.258-0.760) in men and women, respectively. The corresponding results for the MRI measurements of MAT PDFF were 0.487 (range 0.224-0.675) and 0.477 (range 0.238-0.745), respectively. The mean BM volume fractions were 0.122 (range 0.073-0.187) in men and 0.117 (range 0.053-0.187) in women, respectively.

Correlation and agreement of adipose tissue measurements

Figure 3A shows the plot of L1-3 MAT PDFF against the L1-3 DLCT Adj-YM volume fraction [$r^2 = 0.698$, $p < .0001$, standard error of the estimate (SEE) = 0.059] for the validation group, and Figure 3B shows the corresponding Bland–Altman plot. As a further comparison of the DLCT and MRI measurements, we plotted both against age for men and women

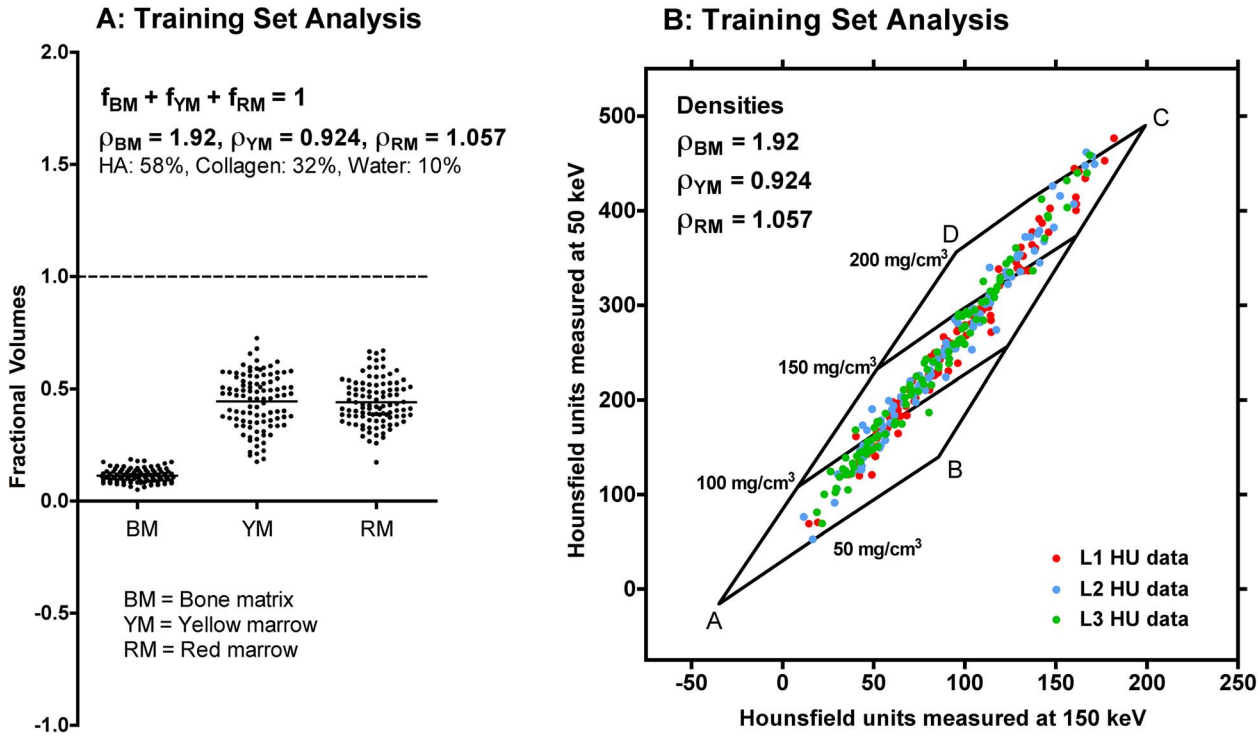

Figure 2. (A) Plots of the fractional volumes of bone matrix (BM), yellow marrow (YM), and red marrow (RM) for the 100 participants in the training set. The composition and density of BM were taken from the paper by Mazess.[15] Mass densities of 0.924 and 1.057 g/cm^3, respectively, for YM and RM gave a mean adjusted YM volume fraction (=YM/[YM + RM]) of 0.50, with ±1.96 SD limits of 0.25 and 0.75, respectively.[15] (B) Quality assurance plot of the 50 and 150 keV mono-energy HU measurements. The rhombus figure ABCD shows the predicted limits for physically realistic solutions of the three-material model with densities of 1.92, 0.924, and 1.057 g/cm^3 for BM, YM, and RM, respectively. Physically realistic solutions of the model should have all three fractional volumes (f_{BM}, f_{YM}, and f_{RM}) within the range 0-1, their sum should add up to 1, and all points with vBMD between 50 and 200 mg/cm^3 should lie inside the rhombus ABCD.

Table 2. Solutions of the three-material model in the training and validation sets.[a]

Parameter	Training set ($n = 100$)		Validation set ($n = 125$)	
	Men ($n = 43$)	Women ($n = 57$)	Men ($n = 44$)	Women ($n = 81$)
DLCT vBMD (mg/cm^3)	131.0 (28.7)	122.8 (34.1)	135.7 (33.2)	130.1 (35.0)
Bone matrix fraction	0.118 (0.026)	0.110 (0.031)	0.122 (0.030)	0.117 (0.031)
Yellow marrow fraction	0.446 (0.112)	0.445 (0.128)	0.416 (0.112)	0.426 (0.116)
Red marrow fraction	0.436 (0.094)	0.445 (0.106)	0.462 (0.092)	0.457 (0.096)
Adjusted yellow marrow fraction[b]	0.503 (0.117)	0.497 (0.132)	0.471 (0.115)	0.480 (0.119)
MRI PDFF	-	-	0.487 (0.103)	0.477 (0.109)

Results expressed as the mean with the SD in parentheses. [a]Results for the training and validation sets calculated using the model parameters in Table S1. [b]Adjusted yellow marrow fraction is the volume of YM as a fraction of the total marrow volume. Abbreviations: DLCT, dual-layer spectral CT; PDFF, proton density fat fraction; vBMD, volumetric BMD.

separately (Figure 4). Linear regression analysis showed a statistically significant trend for the Adj-YM fraction to increase with age in both sexes (all $p < .0001$). The difference in the slopes between the DLCT and MRI plots was not statistically significant in either sex (women: $p = .152$; men: $p = .545$). In addition, both the DLCT and MRI data showed a gradient in MAT measurements down the lumbar spine similar to that reported by Baum et al.[23] In the validation set, mean PDFF (SEM) in L1, L2, and L3 was 0.444 (0.010), 0.484 (0.010), and 0.513 (0.010), respectively. Corresponding results for the DLCT measurements were 0.453 (0.011), 0.478 (0.011), and 0.500 (0.011), respectively.

Figure 5 shows similar plots of DLCT L1-3 vBMD and SEQCT L1-3 vBMD against age. In both sexes, the SEQCT plot showed a steeper decrease with age than the DLCT plot, although the difference was statistically significant only for women ($p = .0059$) (men: $p = .171$).

Relationship between DLCT and SEQCT vBMD measurements

Simple linear regression analysis between SEQCT L1-3 vBMD and DLCT L1-3 vBMD for the 125 participants in the validation set gave the following relationship (coefficient of determination $r^2 = 0.960$, $p < .0001$, SEE = 10.0 mg/cm^3) (Figure 6A):

$$\text{SEQCT L1} - 3\ \text{vBMD}\ \left(\text{mg/cm}^3\right) = 1.414^{*}\text{DLCT L1} - 3\ \text{vBMD}\ \left(\text{mg/cm}^3\right) - 52.2. \quad (1)$$

The difference between DLCT and SEQCT vBMD correlated strongly with the Adj-YM volume fraction with the following relationship (coefficient of determination $r^2 = 0.821$,

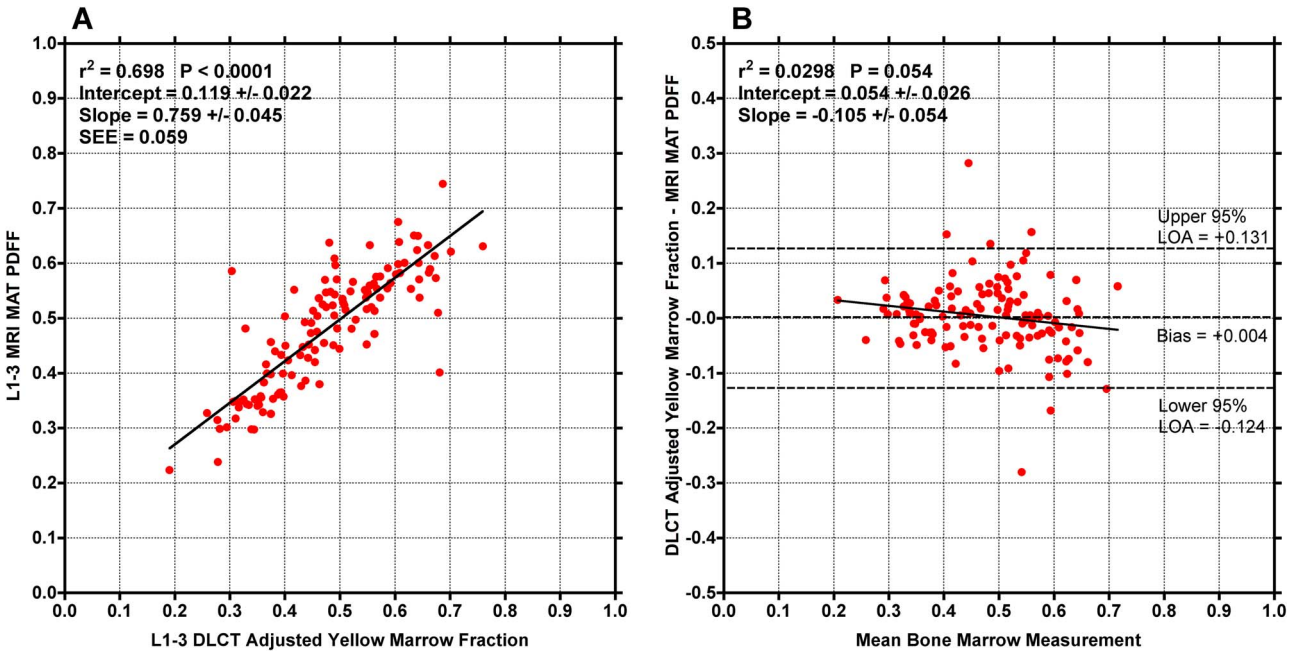

Figure 3. (A) Plot of L1-3 MRI bone marrow proton density fat fraction (PDFF) against L1-3 DLCT measurements of the adjusted yellow marrow volume fraction [Adj-YM = YM/(YM + RM)] for the 125 participants in the validation set. (B) Bland–Altman plot of the same data. The solid straight lines show the results of linear regression analysis.

$p < .0001$) (Figure 6B):

$$\text{DLCT} - \text{SEQCT L1} - 3\ \text{vBMD}\ (\text{mg/cm}) = 133.8^{*}\text{Adj} - \text{YM fraction} - 66.3. \quad (2)$$

Multiple linear regression analysis gave the following equation for predicting SEQCT vBMD from DLCT vBMD and the Adj-YM volume fraction (coefficient of determination $r^2 = 0.989$, $p < .0001$, SEE = 5.2 mg/cm^3) (Figure 6C):

$$\text{SEQCT L1} - 3\ \text{vBMD}\ \left(\text{mg/cm}^3\right) = 1.201^{*}\text{DLCT L1} - 3\ \text{vBMD}\ \left(\text{mg/cm}^3\right) - 95.6^{*}\text{Adj} - \text{YM Fraction} + 21.6. \quad (3)$$

Diagnostic performance of DLCT-derived vBMD

Table 3 lists the values of sensitivity, specificity, PPV, and NPV for different thresholds of DLCT L1-3 vBMD to predict osteoporosis diagnosed by SEQCT. DLCT thresholds of 95, 100, and 105 mg/cm^3 gave sensitivities and specificities of 75.0/98.1%, 100.0/94.3%, and 100.0/87.6%, respectively, for predicting osteoporosis (AUROC = 0.986; 95% CI: 0.949-1.0). Table 4 lists similar values for DLCT vBMD to predict either osteopenia or osteoporosis diagnosed by SEQCT. DLCT thresholds of 110, 120, and 130 mg/cm^3 gave sensitivities and specificities of 80.8/98.6%, 94.2/93.2%, and 100.0/84.9%, respectively, for predicting osteopenia or osteoporosis (AUROC = 0.991; 95% CI: 0.972-1.0). The difference between 2 AUROC areas was not statistically significant ($p = .81$). The inter-observer reliabilities (ICC) between 2 radiologists for the vBMD measurements were 0.999 and 1.000 for DLCT and SEQCT, respectively.

The independent estimates of the densities of YM and RM obtained by matching the DLCT Adj-YM volume fractions to the MRI PDFF measurements gave results consistent with the densities derived from the training set using bone histology data (Figure S3).

Discussion

Dual-energy CT applications for measuring spine bone density, such as DLCT, have the advantage that they can measure the composition of bone marrow as well as bone mineral content.[24–28] In principle, provided that the application yields sufficiently accurate measurements of MAT, vBMD measurements made using dual-energy CT should be more accurate than measurements made using SEQCT. Our study showed good correlation and reasonable agreement between the DLCT Adj-YM fraction and MRI measurements of MAT PDFF, as demonstrated by scatter and Bland–Altman plots. In addition, DLCT vBMD had good sensitivity, specificity, and AUROC for predicting osteoporosis and osteopenia identified by SEQCT.

There are two reasons why variations in the Adj-YM fraction in vertebral trabecular bone may cause errors in SEQCT vBMD measurements.[29] First, adipose tissue has a lower effective atomic number than lean tissue, reducing the photoelectric contribution to the mass attenuation coefficient. Second, adipose tissue has a lower physical density than lean tissue, reducing the mass of material in each unit volume attenuating the X-ray beam, thereby further reducing the linear attenuation coefficient.

The study reported here has involved three alternative methods of quantifying MAT in the spine, MRI PDFF, dual-energy CT, and bone histology that measure distinctly different aspects of bone marrow.[30,31] While many studies show that these three measurements are reasonably well correlated,

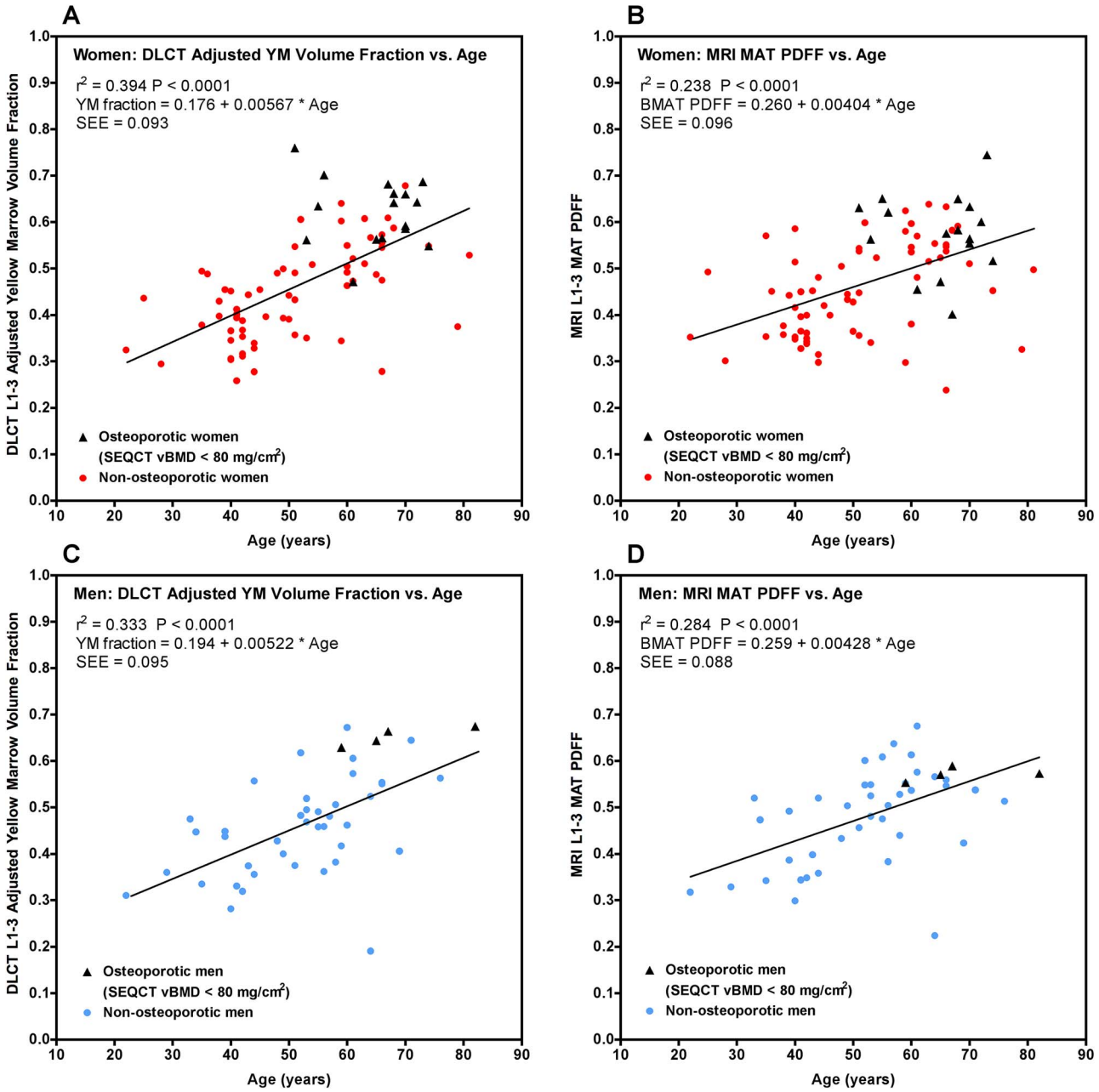

Figure 4. (A) Plot of the L1-3 DLCT measurements of the adjusted yellow marrow volume fraction (=YM/[YM + RM]) against age for the 81 women in the validation set. (B) A similar plot of the MRI measurements of bone marrow proton density fat fraction (PDFF) against age for the same women. (C) Plot of the L1-3 DLCT measurements of the adjusted yellow marrow volume fraction against age for the 44 men in the validation set. (D) A similar plot of the MRI measurements of PDFF against age for the same men. The straight lines show the results of linear regression analysis.

Table 3. Diagnostic performance of DLCT L1-3 vBMD for predicting osteoporosis.[a]

Non-contrast DLCT L1-3 vBMD (mg/cm^3)	Sensitivity (%)	Specificity (%)	PPV (%)	NPV (%)
<85	8/20 (40.0)	105/105 (100.0)	8/8 (100.0)	105/117 (89.7)
<90	11/20 (55.0)	105/105 (100.0)	11/11 (100.0)	105/114 (92.1)
<95	15/20 (75.0)	103/105 (98.1)	15/17 (88.2)	103/108 (95.4)
<100	20/20 (100.0)	(99/105 (94.3)	20/26 (76.9)	99/99 (100.0)
<105	20/20 (100.0)	92/105 (87.6)	20/33 (60.6)	92/92 (100.0)

Data expressed as numerator and denominator, with percentages in parentheses. [a]Defined by a SEQCT L1-3 vBMD <80 mg/cm^3. Abbreviations: NPV, negative predictive value; PPV, positive predictive value; vBMD, volumetric BMD.

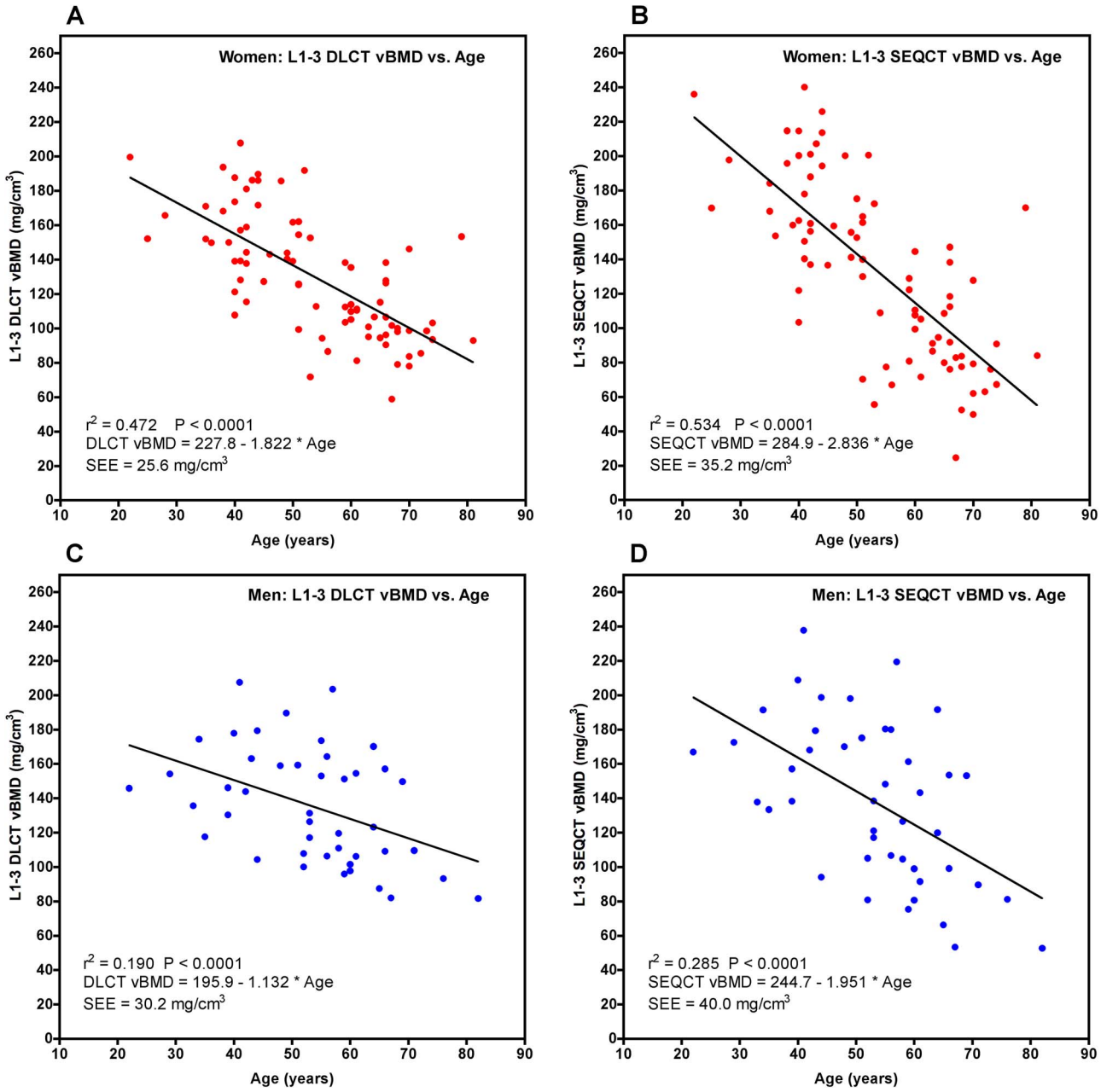

Figure 5. (A) Plot of the L1-3 DLCT measurements of spine vBMD against age for the 81 women in the validation set. (B) A similar plot of the L1-3 SEQCT measurements of spine vBMD against age for the same women. (C) Plot of the L1-3 DLCT measurements of spine vBMD against age for the 44 men in the validation set. (D) A similar plot of the L1-3 SEQCT measurements of spine vBMD against age for the same men. The straight lines show the results of linear regression analysis.

Table 4. Diagnostic performance of DLCT L1-3 vBMD for predicting osteopenia or osteoporosis.[a]

Non-contrast DLCT L1-3 vBMD (mg/cm^3)	Sensitivity (%)	Specificity (%)	PPV (%)	NPV (%)
<100	26/52 (50.0)	73/73 (100.0)	26/26 (100.0)	73/99 (73.7)
<105	33/52 (63.5)	73/73 (100.0)	33/33 (100.0)	73/92 (79.3)
<110	42/52 (80.8)	72/73 (98.6)	42/43 (97.7)	72/82 (87.8)
<115	47/52 (90.4)	71/73 (97.3)	47/49 (95.9)	71/76 (93.4)
<120	49/52 (94.2)	68/73 (93.2)	49/54 (90.7)	68/71 (95.8)
<125	51/52 (98.1)	68/73 (93.2)	51/56 (91.1)	68/69 (98.6)
<130	52/52 (100.0)	62/73 (84.9)	52/63 (82.5)	62/62 (100.0)

Data expressed as numerator and denominator, with percentages in parentheses. [a]Defined by a SEQCT L1–3 vBMD <120 mg/cm^3. Abbreviations: NPV, negative predictive value; PPV, positive predictive value; vBMD, volumetric BMD.

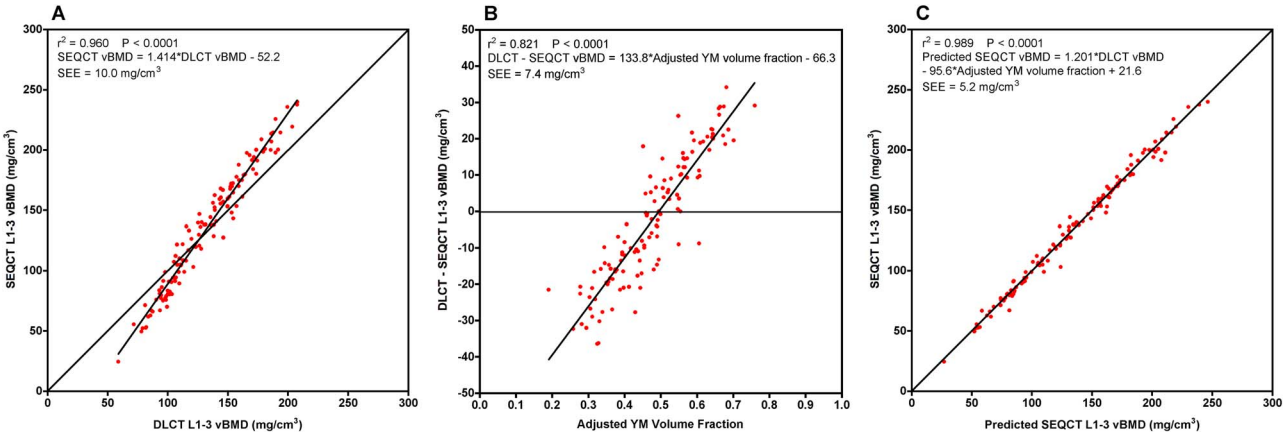

Figure 6. (A) Plot of the SEQCT measurements of L1-3 vBMD against the DLCT L1-3 vBMD measurements for the 125 participants in the validation set. (B) Plot of the difference between DLCT and SEQCT measurements of L1-3 vBMD against the adjusted yellow marrow volume fraction. (C) Plot of SEQCT measurements of L1-3 vBMD against the values predicted by a multiple linear regression model using DLCT BMD and the adjusted yellow marrow volume fraction as the independent variables.

they should not be regarded as equivalent. PDFF is considered the most practical MR-based biomarker for assessing fat concentration in tissue[32] and is the most widely used measurement in imaging studies.[33]

It is important to note that MRI-measured PDFF essentially compares the proton density of free water molecules (ie, water not bound to macromolecules) with the proton density of fat molecules. In contrast, bone histology and dual-energy CT (DLCT) measurements primarily focus on the volume fraction of MAT. PDFF is defined as the ratio of the fat signal from hydrogen atoms to the total signal from both fat and water,[34] which represents a significant difference in measurement principles compared to bone histology and DLCT.

The key distinction lies in the fact that the "free water" in PDFF refers specifically to unbound water molecules with mobile protons that can be detected by conventional MRI sequences. This distinction is crucial because RM contains not only free water but also bound water–water molecules tightly associated with proteins, cellular structures, or the BM. The T2 relaxation times of bound water protons are significantly shortened, making their signals largely undetectable in standard MRI acquisitions. As a result, PDFF measurements may systematically underestimate the total water content in RM due to the omission of bound water contributions. This limitation must be carefully considered when interpreting PDFF results.

Single-voxel magnetic resonance spectroscopy (1H-MRS) is considered the gold standard non-invasive technique for the in vivo measurement of PDFF.[14] However, MRS is time-consuming and technically demanding, and therefore simpler techniques such as the 6-point Q-Dixon method used in the present study are widely used and show a good correlation and concordance with 1H-MRS.[14,35–37] The PDFF results for lumbar spine MAT reported here are similar to those published by other authors.[14,23,35–38] In addition, PDFF measurements in the lumbar spine using the Dixon technique in ex vivo studies have been shown to be well correlated with and comparable to bone histology measurements of the YM fraction[39] and bone marrow cellularity.[40]

A few previous studies have directly compared dual-energy CT with MRI PDFF measurements in the lumbar spine. These include an ex vivo study reported by Arentsen et al.[39] and the in vivo study published by Bredella et al.[41] Despite the differences in technology, both these studies found not only good correlation but also reasonably good numerical agreement. Nevertheless, some caution is necessary in interpreting the results in Figure 3. As noted above, while DLCT and MRI PDFF measurements both respond to the fat content of bone marrow, they differ significantly in the way they respond to the fat-free content. While MRI measures the fat-free content in terms of the water signal, DLCT measures it in terms of the X-ray attenuation of the fat-free tissue, which includes both water and non-aqueous components, including protein and minerals. These latter contribute to the X-ray attenuation coefficient, but not to the MRI signal.

Although other studies have applied the three-material model to DLCT scans of clinical cohorts,[8,9,18,42,43] these cohorts have generally been small, and the reports have not included information about the fractional volumes of YM and RM. However, it is important to demonstrate that the models used in these studies yield physiologically realistic values of the Adj-YM volume fraction. Models that produce YM or RM volume fractions that are either negative or greater than one will also result in errors in the vBMD results. We undertook the study described here because of our experience with one such software application that produced negative values of the YM volume fraction in a large majority of patients. Therefore, the aims of the present study were to develop a three-material model that ensured realistic results for the YM and RM volume fractions and to compare the measurements of the Adj-YM fraction with MRI measurements of MAT PDFF. As far as we are aware, ours is the first paper to address this question, which is important for the assessment of the reliability of dual-energy CT measurements of spine vBMD.

To develop a realistic three-material model that avoided negative values of the YM volume fraction and gave a population distribution of the Adj-YM fraction compatible with human data,[15] it was necessary to set the density of RM to 1.057 g/cm^3. We note that this is higher than the generally accepted figure for RM density (1.02 or 1.03 g/cm^3).[15,19] For this reason, we examined alternative strategies for adjusting the model to the training set data other than varying the YM and RM densities. Other possibilities we investigated were: (1) varying the mono-energy keV values from their nominal values of 50 and 150 keV, (2) varying the elemental composition of RM by adjusting the effective atomic number

(Z_{eff}) and electron density (N_e, units cm^{-3}), and (3) varying the mass densities of hydroxyapatite and collagen from their nominal values.[15] Of the above, only an increase in electron density (equivalent in its effect to an increase in mass density) provided a viable alternative mechanism for avoiding solutions of the three-material model with negative YM volume fractions. We note that in Figure 2B the requirement to set the RM density to 1.057 g/cm^3 arises from the need to explain the high energy 150 keV HU measurements, an energy where Compton scattering and its dependence on electron density is the dominant factor accounting for X-ray attenuation. The requirement of our model for a higher-than-expected RM density therefore relates directly to the higher than expected 150 keV HU measurements and the requirement to avoid unrealistic values of the YM and RM volume fractions as illustrated in Figure S2.

Despite the above disparity, the three-material model proposed here has considerable strengths. The BM, YM, and RM fractional volumes in the individual L1, L2, and L3 vertebrae in all 225 participants in the training and validation sets were between zero and one. We have shown that DLCT scans can provide measurements of the Adj-YM volume fraction in the lumbar vertebrae that are consistent and well correlated with MRI measurements of PDFF. In addition, the model reproduced the expected age variation of MAT and vBMD in both men and women and the variations in PDFF down the lumbar spine.[23,44] Given the long history of discussion of the errors in BMD measurements caused by adipose tissue, there is a compelling argument for thinking that a CT method of measuring vBMD that allows for the MAT content of vertebral trabecular bone will also yield more accurate BMD measurements. The model also throws new light on how the difference between DLCT and SEQCT vBMD measurements varies with the Adj-YM fraction. After adjustment for Adj-YM, the SEE between DLCT and SEQCT vBMD measurements is 5.2 mg/cm^3.

The limitations of this study include the uncertainty about the exact relationship between dual-energy CT estimates of MAT, modern 6-point Q-Dixon measurements of MRI PDFF, and the bone histology studies used to calibrate our model. These are three very different types of measurement, and the relationship between them requires further clarification. The study was conducted with Chinese participants, and other ethnic groups might produce different findings. Measurements of more subjects over a wide range of ages would give improved information about the variation of DLCT Adj-YM and vBMD with age in each sex compared with MRI and SEQCT. Finally, our study only included the three lumbar vertebrae L1, L2, and L3. It is unclear whether the same model can be applied to other vertebrae.

In conclusion, we have trained and assessed a three-material model for analyzing DLCT spine BMD scans that correlates with MRI measurements of PDFF and reproduces the expected variations of the Adj-YM fraction and vBMD with age. The data provide new insight into how the difference between DLCT and SEQCT vBMD measurements depends on the Adj-YM fraction.

Acknowledgments

The authors express their gratitude to all the participants who volunteered for this study and study personnel who contributed to its success.

Author contributions

Fengyun Zhou and Glen M. Blake contributed equally and are co-first authors.

Fengyun Zhou (Data curation, Formal analysis, Methodology, Resources, Validation, Visualization, Writing—original draft), Glen M. Blake (Data curation, Formal analysis, Investigation, Methodology, Resources, Validation, Visualization, Writing—original draft, Writing—review & editing), Zhe Guo (Conceptualization, Formal analysis, Methodology, Validation, Writing—review & editing), Wenshuang Zhang (Conceptualization, Investigation, Resources, Visualization, Writing—review & editing), Yi Yuan (Data curation, Methodology, Formal analysis, Writing—review & editing), Yandong Liu (Data curation, Formal analysis, Writing—review & editing), Jian Geng (Data curation, Formal analysis, Writing—review & editing), Bo Hu (Data curation, Writing—review & editing), Kangkang Ma (Data curation, Writing—review & editing), Zitong Cheng (Data curation, Writing—review & editing), Qingyu Zhang (Data curation, Writing—review & editing), Dong Yan (Data curation, Formal analysis, Writing—review & editing), Xiaoguang Cheng (Conceptualization, Data curation, Formal analysis, Funding acquisition, Investigation, Methodology, Project administration, Resources, Writing—review & editing), and Ling Wang (Conceptualization, Data curation, Formal analysis, Funding acquisition, Investigation, Methodology, Project administration, Resources, Supervision, Validation, Writing—review & editing)

Supplementary material

Supplementary material is available at *JBMR Plus* online.

Funding

This work was supported by Beijing Municipal Public Welfare Development and Reform Pilot Project for Medical Research Institutes (JYY2023-8, JYY2023-11), Beijing Physician Scientist Training Project (BJPSTP-2024-08), Beijing Jishuitan Research Funding (JSTYC202207), Beijing Municipal Health Commission (BJRITO-RDP-2024), the National Natural Science Foundation of China (Grant 82371957, 82371956).

Conflicts of interest

The authors declared no potential conflicts of interest concerning the research, authorship, and/or publication of this article. All authors contributed to the study's conception and design. Material preparation, data collection, and analysis were performed by Fengyun Zhou, Glen M. Blake, Zhe Guo, Wenshuang Zhang, Yi Yuan, Yandong Liu, Jian Geng, Bo Hu, Kangkang Ma, Zitong Cheng, Qingyu Zhang, Dong Yan, Xiao Guang Cheng, Ling Wang. All authors commented on previous versions of the manuscript. All authors read and approved the final manuscript.

Data availability

Study data will be made available on reasonable request to one of the corresponding authors.

References

1. Lee SJ, Anderson PA, Pickhardt PJ. Predicting future hip fractures on routine abdominal CT using opportunistic osteoporosis screening measures: a matched case-control study. *AJR Am J Roentgenol*. 2017;209(2):395-402. https://doi.org/10.2214/AJR.17.17820
2. Donohue D, Decker S, Ford J, et al. Opportunistic CT screening for osteoporosis in patients with pelvic and acetabular trauma: technique and potential clinical impact. *J Orthop Trauma*.

2018;32(8):408-413. https://doi.org/10.1097/BOT.0000000000001231
3. Fuggle NR, Curtis EM, Ward KA, Harvey NC, Dennison EM, Cooper C. Fracture prediction, imaging and screening in osteoporosis. *Nat Rev Endocrinol*. 2019;15(9):535-547. https://doi.org/10.1038/s41574-019-0220-8
4. Buenger F, Eckardt N, Sakr Y, Senft C, Schwarz F. Correlation of bone density values of quantitative computed tomography and Hounsfield units measured in native computed tomography in 902 vertebral bodies. *World Neurosurg*. 2021;151:e599-e606. https://doi.org/10.1016/j.wneu.2021.04.093
5. Rassouli N, Etesami M, Dhanantwari A, Rajiah P. Detector-based spectral CT with a novel dual-layer technology: principles and applications. *Insights Imaging*. 2017;8(6):589-598. https://doi.org/10.1007/s13244-017-0571-4
6. Mei K, Schwaiger BJ, Kopp FK, et al. Bone mineral density measurements in vertebral specimens and phantoms using dual-layer spectral computed tomography. *Sci Rep*. 2017;7(1):17519. https://doi.org/10.1038/s41598-017-17855-4
7. van Hamersvelt RW, Schilham AMR, Engelke K, et al. Accuracy of bone mineral density quantification using dual-layer spectral detector CT: a phantom study. *Eur Radiol*. 2017;27(10):4351-4359. https://doi.org/10.1007/s00330-017-4801-4
8. Roski F, Hammel J, Mei K, et al. Bone mineral density measurements derived from dual-layer spectral CT enable opportunistic screening for osteoporosis. *Eur Radiol*. 2019;29(11):6355-6363. https://doi.org/10.1007/s00330-019-06263-z
9. Van Hedent S, Su K-H, Jordan DW, et al. Improving bone mineral density assessment using spectral detector CT. *J Clin Densitom*. 2019;22(3):374-381. https://doi.org/10.1016/j.jocd.2018.10.004
10. Hu T, Yang X, Gao L, et al. Feasibility analysis of low-dose CT with asynchronous quantitative computed tomography to assess vBMD. *BMC Med Imaging*. 2023;23(1):149. https://doi.org/10.1186/s12880-023-01115-1
11. Fedorov A, Beichel R, Kalpathy-Cramer J, et al. 3D slicer as an image computing platform for the quantitative imaging network. *Magn Reson Imaging*. 2012;30(9):1323-1341. https://doi.org/10.1016/j.mri.2012.05.001
12. Grimm A, Meyer H, Nickel MD, et al. Evaluation of 2-point, 3-point, and 6-point Dixon magnetic resonance imaging with flexible echo timing for muscle fat quantification. *Eur J Radiol*. 2018;103:57-64. https://doi.org/10.1016/j.ejrad.2018.04.011
13. van Vucht N, Santiago R, Lottmann B, et al. The Dixon technique for MRI of the bone marrow. *Skeletal Radiol*. 2019;48(12):1861-1874. https://doi.org/10.1007/s00256-019-03271-4
14. Lee SH, Yoo HJ, Yu S-M, Hong SH, Choi J-Y, Chae HD. Fat quantification in the vertebral body: comparison of modified Dixon technique with single-voxel magnetic resonance spectroscopy. *Korean J Radiol*. 2019;20(1):126-133. https://doi.org/10.3348/kjr.2018.0174
15. Mazess RB. Errors in measuring trabecular bone by computed tomography due to marrow and bone composition. *Calcif Tissue Int*. 1983;35(1):148-152. https://doi.org/10.1007/BF02405022
16. Nickoloff EL, Feldman F, Atherton JV. Bone mineral assessment: new dual-energy CT approach. *Radiology*. 1988;168(1):223-228. https://doi.org/10.1148/radiology.168.1.3380964
17. Gassert FT, Hammel J, Hofmann FC, et al. Detection of bone marrow edema in patients with osteoid osteoma using three-material decomposition with dual-layer spectral CT. *Diagnostics (Basel)*. 2021;11(6):953. https://doi.org/10.3390/diagnostics11060953
18. Koch V, Hokamp NG, Albrecht MH, et al. Accuracy and precision of volumetric bone mineral density assessment using dual-source dual-energy versus quantitative CT: a phantom study. *Eur Radiol Exp*. 2021;5(1):43. https://doi.org/10.1186/s41747-021-00241-1
19. *ICRU Report 46, Photon, Electron, Proton and Neutron Interaction Data for Body Tissues*. Bethesda, MD: International Commission on Radiation Units and Measurements (ICRU). https://www.icru.org/report/photon-electron-proton-and-neutron-interaction-data-for-body-tissues-report-46/
20. PubChem Compound Summary. *Collagen I, Alpha Chain (98–110)*. PubChem; Bethesda, MD: National Center for Biotechnology Information (NCBI). https://pubchem.ncbi.nlm.nih.gov/compound/Collagen-I_-alpha-chain-_98-110
21. NIST. *X-Ray Mass Attenuation Coefficients - Introduction*. Gaithersburg, MD: National Institute of Standards and Technology. https://physics.nist.gov/PhysRefData/XrayMassCoef/intro.html
22. Expert Panel on Musculoskeletal Imaging, Ward RJ, Roberts CC, Bencardino JT, et al. ACR appropriateness criteria osteoporosis and bone mineral density. *J Am Coll Radiol*. 2017;14(5S):S189-S202. https://doi.org/10.1016/j.jacr.2017.02.018
23. Baum T, Rohrmeier A, Syväri J, et al. Anatomical variation of age-related changes in vertebral bone marrow composition using chemical shift encoding-based water-fat magnetic resonance imaging. *Front Endocrinol (Lausanne)*. 2018;9:141. https://doi.org/10.3389/fendo.2018.00141
24. Laval-Jeantet AM, Cann CE, Roger B, Dallant P. A postprocessing dual energy technique for vertebral CT densitometry. *J Comput Assist Tomogr*. 1984;8(6):1164-1167. https://doi.org/10.1097/00004728-198412000-00024
25. Mallinson PI, Coupal TM, McLaughlin PD, Nicolaou S, Munk PL, Ouellette HA. Dual-energy CT for the musculoskeletal system. *Radiology*. 2016;281(3):690-707. https://doi.org/10.1148/radiol.2016151109
26. Yuh I, Yamamoto I, Ohnaka Y, et al. Determination of vertebral fracture threshold by measuring bone mineral content in the lumbar vertebrae. *Nihon Igaku Hoshasen Gakkai Zasshi*. 1992;52(2):217-222
27. Adams JE, Chen SZ, Adams PH, Isherwood I. Measurement of trabecular bone mineral by dual energy computed tomography. *J Comput Assist Tomogr*. 1982;6(3):601-607. https://doi.org/10.1097/00004728-198206000-00028
28. Vetter JR, Perman WH, Kalender WA, Mazess RB, Holden JE. Evaluation of a prototype dual-energy computed tomographic apparatus. II. Determination of vertebral bone mineral content. *Med Phys*. 1986;13(3):340-343. https://doi.org/10.1118/1.595951
29. Laval-Jeantet AM, Roger B, Bouysee S, Bergot C, Mazess RB. Influence of vertebral fat content on quantitative CT density. *Radiology*. 1986;159(2):463-466. https://doi.org/10.1148/radiology.159.2.3961178
30. Tratwal J, Labella R, Bravenboer N, et al. Reporting guidelines, review of methodological standards, and challenges toward harmonization in bone marrow adiposity research. Report of the methodologies working Group of the International Bone Marrow Adiposity Society. *Front Endocrinol (Lausanne)*. 2020;11:65. https://doi.org/10.3389/fendo.2020.00065 eCollection 2020
31. Singhal V, Bredella MA. Marrow adipose tissue imaging in humans. *Bone*. 2019;118:69-76. https://doi.org/10.1016/j.bone.2018.01.009
32. Reeder SB, Hu HH, Sirlin CB. Proton density fat-fraction: a standardized MR-based biomarker of tissue fat concentration. *J Magn Reson Imaging*. 2012;36(5):1011-1014. https://doi.org/10.1002/jmri.23741
33. Hu HH, Kan HE. Quantitative proton MR techniques for measuring fat. *NMR Biomed* 2013;26(12):1609–1629. https://doi.org/10.1002/nbm.3025
34. Reeder SB, Hines CD, Yu H, McKenzie CA, Brittain JH. On the definition of fat-fraction for in vivo fat quantification with magnetic resonance imaging. *Proceedings of the 17th Annual Scientific Meeting of the International Society for Magnetic Resonance in Medicine*. 2009;17:211 https://cds.ismrm.org/protected/09MProceedings/PDFfiles/00211.pdf
35. Pei X-J, Lian Y-F, Yan Y-C, et al. Fat fraction quantification of lumbar spine: comparison of T1-weighted two-point Dixon and single-voxel magnetic resonance spectroscopy in diagnosis of multiple myeloma. *Diagn Interv Radiol*. 2020;26(5):492-497. https://doi.org/10.5152/dir.2020.19401
36. Li G, Xu Z, Gu H, et al. Comparison of chemical-shift-encoded water-fat MRI and MR spectroscopy in quantification of

marrow fat in postmenopausal females. *J Magn Reson Imaging*. 2017;45(1):66-73. https://doi.org/10.1002/jmri.25351
37. Lins CF, Salmon CEG, de Souza LA, et al. Six-point DIXON and magnetic resonance spectroscopy techniques in quantifying bone marrow fat in sickle cell disease. *Acad Radiol*. 2022 May;29(5):e73-e81. https://doi.org/10.1016/j.acra.2021.06.006
38. Karampinos DC, Ruschke S, Dieckmeyer M, et al. Quantitative MRI and spectroscopy of bone marrow. *J Magn Reson Imaging*. 2018;47(2):332-353. https://doi.org/10.1002/jmri.25769
39. Arentsen L, Yagi M, Takahashi Y, et al. Validation of marrow fat assessment using noninvasive imaging with histologic examination of human bone samples. *Bone*. 2015;72:118-122. https://doi.org/10.1016/j.bone.2014.11.002
40. MacEwan IJ, Glembotski NE, D'Lima D, et al. Proton density water fraction as a biomarker of bone marrow cellularity: validation in ex vivo spine specimens. *Magn Reson Imaging*. 2014;32(9):1097-1101. https://doi.org/10.1016/j.mri.2014.03.005
41. Bredella MA, Daley SM, Kaira MK, Brown JK, Miller KK, Torriani M. Marrow adipose tissue quantification of the lumbar spine by using dual-energy CT and single-voxel ^{1}H MR spectroscopy: a feasibility study. *Radiology*. 2015;277(1):230-235. https://doi.org/10.1148/radiol.2015142876
42. Li X, Li X, Li J, et al. The accuracy of bone mineral density measurement using dual-energy spectral CT and quantitative CT: a comparative phantom study. *Clin Radiol*. 2020;75(4):320.e9-320.e15. https://doi.org/10.1016/j.crad.2019.11.008
43. Booz C, Hofmann PC, Sedlmair M, et al. Evaluation of bone mineral density of the lumbar spine using a novel phantomless dual-energy CT post-processing algorithm in comparison with dual-energy X-ray absorptiometry. *Eur Radiol Exp*. 2017;1(1):11. https://doi.org/10.1186/s41747-017-0017-2
44. Yu A, Huang M, Wang L, et al. Age and gender differences in vertebral bone marrow adipose tissue and bone mineral density, based on MRI and quantitative CT. *Eur J Radiol*. 2023;159:110669. https://doi.org/10.1016/j.ejrad.2022.110669

JBMR Plus, 2025, 9, ziaf066
https://doi.org/10.1093/jbmrpl/ziaf066
Research Article